Weierstraß-Institut
für Angewandte Analysis und Stochastik
Leibniz-Institut im Forschungsverbund Berlin e. V.

Preprint ISSN 2198-5855

Turbulent coherent structures in a long cavity semiconductor laser near the lasing threshold

Uday Gowda[1,2,3], Amy Roche[1,2,3], Alexander Pimenov[4], Andrei G. Vladimirov[4],

Svetlana Slepneva[1,2,3], Evgeny A. Viktorov[5], Guillaume Huyet[1]

submitted: May 26, 2020

[1] Université Côte d'Azur
CNRS
INPHYNI
Parc Valrose
06108 Nice
France
E-Mail: svetlana.slepneva@inphyni.cnrs.fr
guillaume.huyet@inphyni.cnrs.fr

[2] Centre for Advanced Photonics and Process Analysis and
Department of Physical Sciences
Cork Institute of Technology
T12P928 Cork
Ireland

[3] Tyndall National Institute
University College Cork
Lee Maltings
Dyke Parade
T12R5CP Cork
Ireland

[4] Weierstrass Institute
Mohrenstr. 39
10117 Berlin
Germany
E-Mail: alexander.pimenov@wias-berlin.de
andrei.vladimirov@wias-berlin.de

[5] ITMO University
Kronverkskiy Prospekt 49
197101 Saint Petersburg
Russia
E-Mail: eaviktorov@itmo.ru

No. 2724
Berlin 2020

2010 *Physics and Astronomy Classification Scheme.* 42.55.Px, 42.65.Sf, 42.60.Mi, 42.55.Ah, 02.30.Ks.

Key words and phrases. Coherent structures, turbulence, long cavity laser.

Deutsche Forschungsgemeinschaft (DFG, German Research Foundation) under Germany's Excellence Strategy – The Berlin Mathematics Research Center MATH+ (EXC-2046/1, ID: 390685689), project AA2-3; H2020-MSCA-IF-2017, ICO-FAS (800290); CIT School of Science PhD Scholarship 2018; SFI IPIC (12/RC/2276); H2020-MSCA-RISE-2018 HALT; OPTIMAL, FEDER; Government of the RF (08-08).

Edited by
Weierstraß-Institut für Angewandte Analysis und Stochastik (WIAS)
Leibniz-Institut im Forschungsverbund Berlin e. V.
Mohrenstraße 39
10117 Berlin
Germany

Fax: +49 30 20372-303
E-Mail: preprint@wias-berlin.de
World Wide Web: http://www.wias-berlin.de/

Turbulent coherent structures in a long cavity semiconductor laser near the lasing threshold

Uday Gowda, Amy Roche, Alexander Pimenov, Andrei G. Vladimirov, Svetlana Slepneva, Evgeny A. Viktorov, Guillaume Huyet

Abstract

We report on the formation of novel turbulent coherent structures in a long cavity semiconductor laser near the lasing threshold. Experimentally, the laser emits a series of power dropouts within a roundtrip and the number of dropouts per series depends on a set of parameters including the bias current. At fixed parameters, the drops remain dynamically stable, repeating over many roundtrips. By reconstructing the laser electric field in the case where the laser emits one dropout per round trip and simulating its dynamics using a time-delayed model, we discuss the reasons for long-term sustainability of these solutions. We suggest that the observed dropouts are closely related to the coherent structures of the cubic complex Ginzburg-Landau equation.

1 Introduction

The development of simple one dimensional systems to study the formation of coherent structures is of paramount interest in the investigation of one-dimensional turbulence, and long cavity lasers have been an excellent test-bed for these studies. Indeed, long fiber lasers can exhibit the laminar-turbulent transition [1], while convective Nozaki-Bekki holes (NBH) may deteriorate the coherence of long cavity optical coherence tomography (OCT) lasers [2–4], thus making the problem of formation of turbulent coherent structures in a long cavity laser interesting from the point of view of nonlinear dynamics as well as application. In this Letter we address the question of formation of turbulent coherent structures observed in a long cavity laser near the lasing threshold and investigate the reasons for their sustainability.

The formation of localized structures, such as vortices shedding behind an obstacle, play a cardinal role in the development of turbulence [5]. While turbulence in hydrodynamics usually occurs in three spatial dimensions, optical turbulence is usually observed in the transverse section [6] or in the temporal evolution of the light beam [7–9], and is usually confined in one or two spatial dimensions. From a fundamental viewpoint, the formation of localized structures and the development of turbulence in one-dimensional systems is also an interesting problem since the stability criteria usually depend on the dimension of the system. For example, the topological argument explaining the stability of vortices in 2D dissipative systems does not hold in 1D [10]. Most of the theoretical studies of one dimensional systems have been carried out using the framework of the Complex Ginzburg-Landau Equation (CGLE) [11]:

$$\begin{aligned}\partial_t \mathcal{A}(t,x) = \mathcal{A}(t,x) + (1+ib)\,\partial_x^2 \mathcal{A}(t,x) - \\ - (1+ic)\,|\mathcal{A}(t,x)|^2 \mathcal{A}(t,x),\end{aligned} \tag{1}$$

where $\mathcal{A}(t,x)$ describes the complex amplitude of a wave evolving in time and in space. The real coefficients b and c represent, respectively, the linear, and non-linear wave dispersion. Coherent structures

DOI 10.20347/WIAS.PREPRINT.2724

of the CGLE are stationary or uniformly moving solutions of the form $\mathcal{A}(t,x) = a(x-vt)e^{i\omega t}$. As a special feature of the cubic CGLE, an analytic expression was found by Nozaki and Bekki for hole solutions, which are nowadays referred to as Nozaki-Bekki Holes (NBH) [6]. These solutions are characterised by a localized dip in the field amplitude $|\mathcal{A}|$ that moves with constant speed and emits plane waves with different wave numbers [7, 8]. The stability of NBH has been the subject of numerous theoretical studies [9]. It was found that emitted waves may exhibit a convective or absolute instability in addition to the core instability of the hole. Moreover, the existence of a family of uniformly moving NBH solutions relies on the inner symmetry of the cubic CGLE [10]. Hence, this family is structurally unstable with respect to a general perturbation of the CGLE, e.g., by higher-order terms such as quintic non-linearity [11]. Thus, while NBH were studied in hydrothermal [12] and cardiac waves [13] with the help of the CGLE, discovery of dynamical regimes in real physical systems that can be related to these solutions remains a challenging problem [3].

Here we study the formation of NBH type structures in a long laser operating near the lasing threshold.

2 Setup

The long-cavity laser was realised as shown in Fig. 1. The laser was designed to operate around 1300 nm and comprised of an SOA gain medium and a narrow transmission bandwidth 8.75 GHz tunable filter. A detailed description of all the laser components can be found in [2]. The long cavity mainly comprised of single mode fiber (SMF) pigtails forming a total length of approximately 27 m, corresponding to a round trip time of 136 ns. The filter transmission wavelength was fixed at 1299 nm, i.e. near the zero dispersion point [14]. The dynamics of this long cavity laser has been modelled using a Delay Differential Equations (DDE) model [2]

$$\dot{A}(t) + (\gamma - i\Delta(t))A(t) = \sqrt{\kappa}\gamma e^{(1-i\alpha)G(t-\tau)/2}A(t-\tau), \tag{2}$$

$$\dot{G}(t) = \gamma_g(g_0 - G(t) - (e^{G(t)} - 1)|A|^2(t)), \tag{3}$$

where $A(t)$ is the electric field envelope at the entrance of the SOA section, $G(t)$ is the cumulative saturable gain in this section, the parameter γ is the spectral filter bandwidth. Here, dot corresponds to differentiation with respect to time t and τ is the cavity round trip time. Δ describes the detuning from the central frequency of the filter, $\kappa < 1$ is the round trip attenuation factor due to the linear non-resonant losses in the SOA section and output of radiation from the cavity, α is the linewidth enhancement factor, γ_g is the carrier relaxation rate in SOA, and g_0 is the pump parameter. Previous studies have demonstrated that this DDE model successfully describes the dynamics experimentally observed in hybrid SOA-fiber lasers. In particular, we have demonstrated that near the zero dispersion point, fixed filter transmission and high bias current, the laser can operate either in continuous wavelength (cw) or chaotic turbulent regime [2, 3]. When the central frequency of the filter transmission is periodically modulated at a frequency close to the round trip frequency, the laser displays a sequence of regimes corresponding to stable and turbulent outputs [2] which include the formation of NBH drifting into a turbulent regime [3]. In addition, in the anomalous dispersion regime, the cw regime becomes unstable and the appearance of the Benjamin-Feyr instability [11] can also be captured by adding a polarisation equation describing the chromatic dispersion of the medium [14].

While DDE model (2)-(3) provides a realistic qualitative description of the dynamics of the long-cavity laser, it is worthwhile to note that near the lasing threshold, where the field amplitude $A(t)$ evolves much slower than the carrier density, after adiabatic elimination of the variable G it can be reduced to

the purely diffusive CGLE (1) [15]. In this GGLE the space and time variables x and t correspond to the original time t (fast time scale) and to the round-trip number t/τ (slow time scale), respectively, and the amplitude $\mathcal{A}(t,x)$ satisfies periodic boundary condition in x. The nonlinear dispersion coefficient is given by the linewidth enhancement factor, $c = -\alpha$, and the linear dispersion coefficient proportional to the chromatic dispersion of the medium is equal to zero, $b = 0$, near the zero dispersion point, where the DDE system (2)-(3) is valid. Thus, assuming that the carrier relaxation is sufficiently fast and the pump is sufficiently weak for CGLE approximation to be useful, the further necessary conditions for the existence and stability of NBH are strong nonlinearity $|\alpha| = |c| > 1$ [11] and sufficiently long cavity such that the condition $\gamma\tau\sqrt{g_0 - g_{0,th}} \gg 1$ could be satisfied near the lasing threshold. The latter condition means that sufficiently large number of longitudinal modes necessary for the NBH formation fall within the gain bandwidth. While these conditions can be satisfied in a long-cavity SOA laser, the assumption of weak pump for the validity of CGLE mentioned above remains limiting, because the gain relaxation of SOA is slow and the value of $\frac{\gamma}{\gamma_g} > 1$ is usually high, thus making the discovery and analysis of NBH near the lasing threshold a difficult problem both experimentally and theoretically.

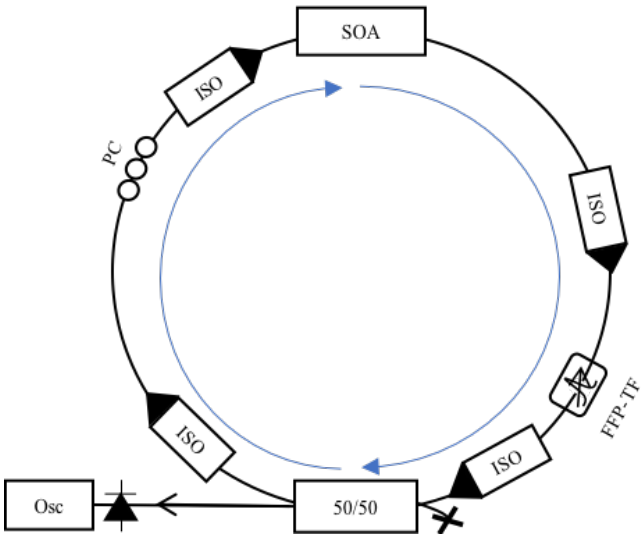

Figure 1: Long cavity laser. SOA, semiconductor optical amplifier; ISO, isolator; FFP-TF, fiber Fabry-Pérot tunable filter; Osc, real-time oscilloscope (12 GHz bandwidth and 40 GSa/s sampling rate); PC, polarisation controller; 50:50 fiber splitter as an output tap coupler. The blue arrows show the direction of light circulation in the cavity.

3 Experimental results

Experimentally, just above threshold, the laser emitted multiple dropouts per roundtrip. Figure 2 (a) shows the intensity of the laser during one roundtrip of 136 ns, recorded using a real-time oscilloscope and 12 GHz photodetectors, and shows multiple, large-amplitude, irregular dropouts of intensity. As the bias current was increased the amount of dropouts per roundtrip time decreased. Figure 2 (b) and (c) both show four subsequent cavity round trips, each with a decreased amount of dropouts corresponding to their associated bias currents. Figure 2 (d) shows a 10 ns zoom of a single drop, demonstrating that a drop exhibits several internal oscillations and lasts approximately 1 ns. These oscillations vary in an irregular manner from one round trip to another.

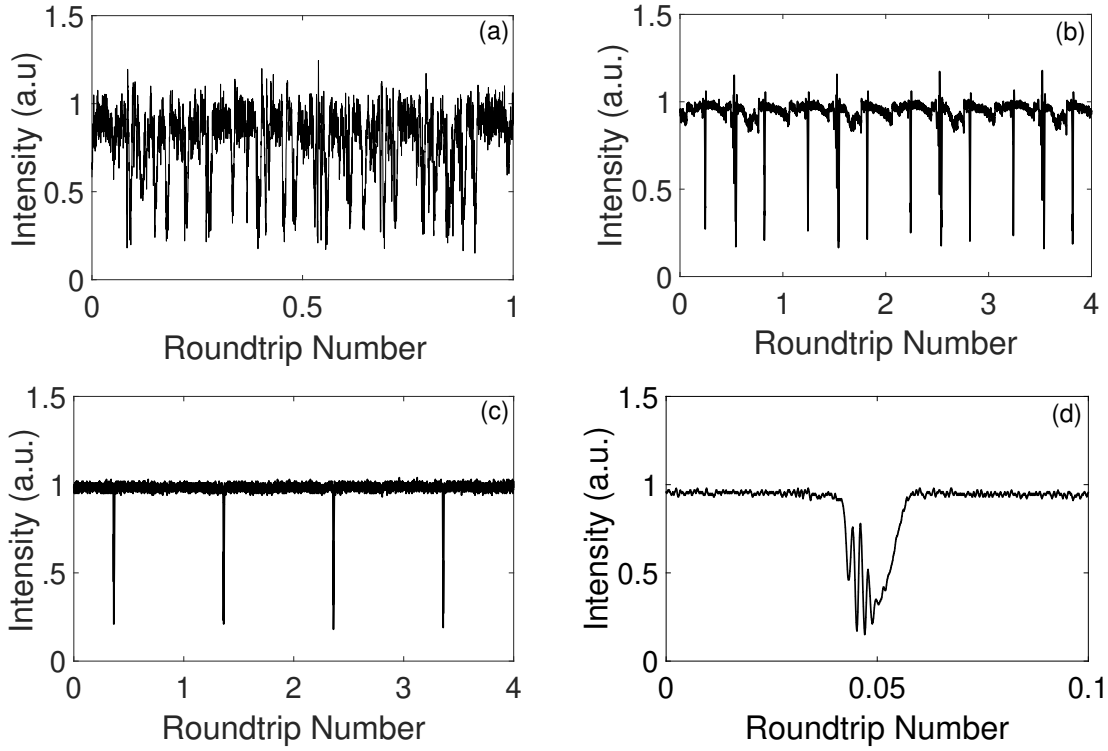

Figure 2: Evolution of the laser intensity dynamics at various ratios of bias current I_b to threshold current I_{th} values for (a) one roundtrip at $I_b/I_{th} = 1.1$; (b) five roundtrips at $I_b/I_{th} = 1.28$ and (c) five roundtrips at $I_b/I_{th} = 1.56$. (d) shows a 10 ns zoom of a single drop. The intensity is normalised to the average of the cw level.

Figure 3 (a) shows a 2D diagram of the evolution of the laser intensity during one roundtrip, containing a single dropout which remains stable for more than 1500 roundtrips. The number of roundtrips recorded was limited by the maximum memory of the oscilloscope. Figure 3 (b) shows the time trace corresponding to the first roundtrip, where the drop is followed by two small intensity fluctuations. On the 2D diagram, the blue line corresponds to the evolution of the dropout, while the dark yellow lines indicate small intensity fluctuations around the cw solution. These small intensity fluctuations also remain stable in the cavity but they propagate at a speed exceeding the speed of the drop. This indicates that the group velocity of the drop is smaller than that of the cw solution.

Figure 4 (a) provides an insight on the intensity dynamics which can occur within a drop. The intensity within the drop oscillates (Figure 4 (b)) and occasionally, one oscillation cycle can separate and propagate away form the main part of the drop (Figure 4 (c)). This seeds a separate unstable structure, which consists of a narrow drop-peak pair. As the pair moves away from the main drop, the amplitude of intensity fluctuations decreases (Figure 4 (d)), and the pair eventually disappears.

Next, the evolution of the phase of the laser in the frame of the stable narrow linewidth reference laser is measured using the interferometric technique [16] previously applied to explain the dynamics of long cavity fast frequency sweeping lasers [3]. Before the dropout, the measured phase increases linearly with time (Fig. 5(a)), indicating that the laser operates in a single frequency regime. The positive slope of the phase corresponds to the frequency difference between the long cavity laser and the reference laser. During the drop the rate abruptly increases corresponding to a 3.7 GHz blue shift of the laser frequency. After the drop, the slope of the phase returns to the value similar to the original. Such a

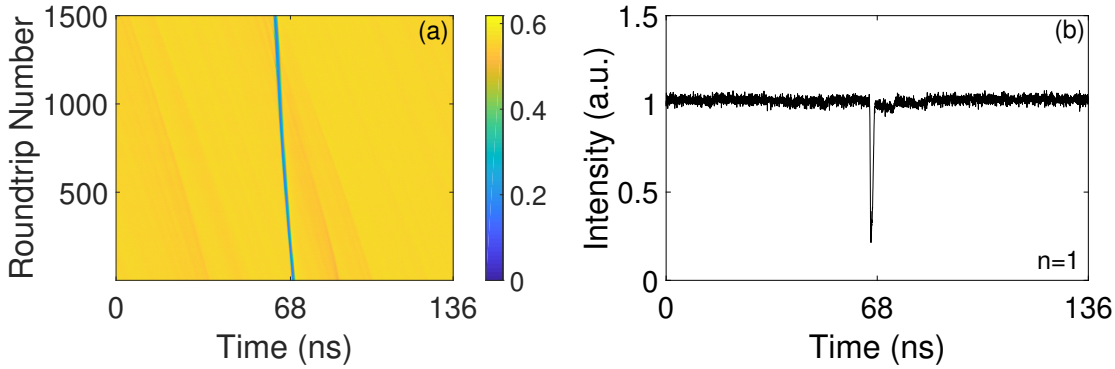

Figure 3: (a) Temporal evolution of a single drop per round trip for over 1500 round trips. The color bar corresponds to the intensity in arbitrary units (a.u.); the time axis shows one cavity round trip of 136 ns. The TLS is the blue trace and small dips in intensity are the dark yellow traces. (b) The laser intensity time trace for the first roundtrip.

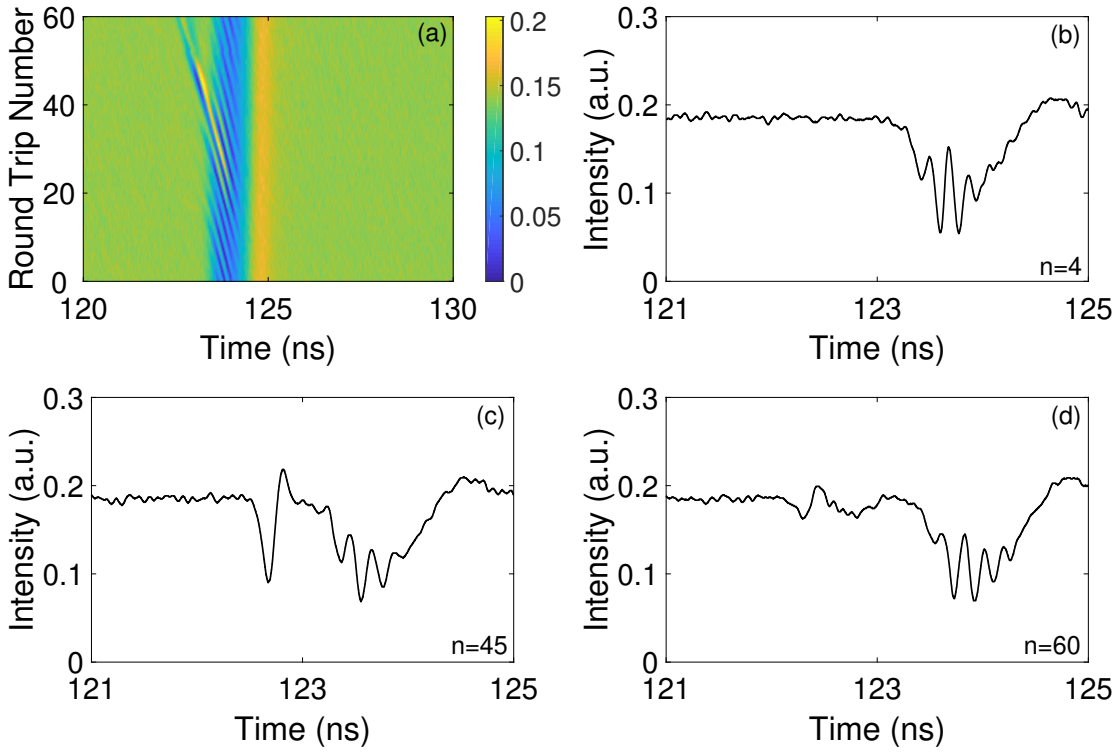

Figure 4: An example of a drop seeding a drop-peak pair. (a) 2D diagram zoomed on one drop demonstrates 10 ns of 136 ns roundtrip, the color bar corresponds to the intensity in arbitrary units. In this diagram, the appearance of the drop-peak pair can be clearly identified at roundtrip 40. During the next 10 roundtrips the pair drifts away from the main drop and destabilises. Corresponding intensity time traces for roundtrip 4 (b); roundtrip 45 when the pair is well separated from the main part of the drop (c) and roundtrip 60 when the pair destabilises (d).

blue shift can be explained from semiconductor laser physics: the power dropout leads to an increase of the gain of the SOA resulting in a frequency shift of the laser due to the linewidth enhancement factor of the SOA. This frequency shift is behind the experimental sustainability of the dropouts. The

frequency shift of 3.7 GHz corresponds to approximately the half of the filter transmission bandwidth, thus leading to a substantial drop modification by the filter, as explained in Fig. 5(b), showing the intensity measured before and after the filter. Such a behaviour indicates that the the dropouts are stable when the frequency shift due to the nonlinear dispersion is larger than the filter bandwidth.

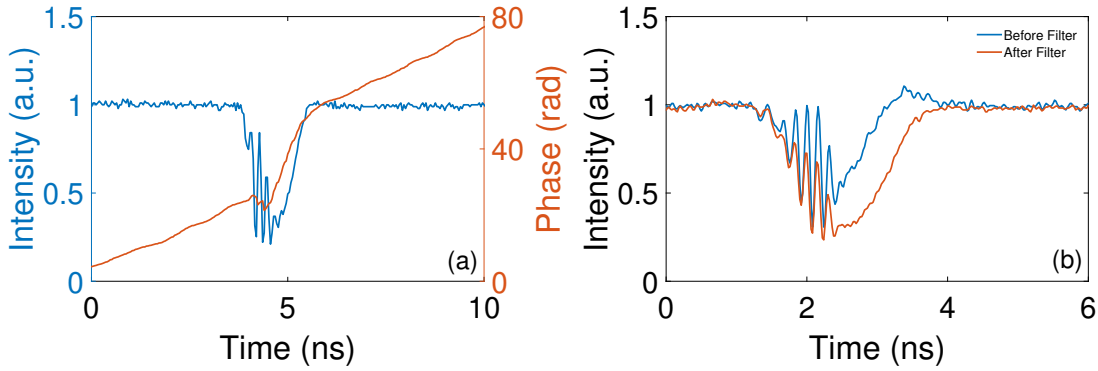

Figure 5: (a) Intensity (blue) and phase (orange) of a single dropout. (b) Intensity of the dropout measured before (blue curve) and after (orange curve) the filter. An additional fiber coupler was introduced before the filter in the cavity (Fig. 1) Each intensity time trace is normalises to the average of the corresponding cw level.

4 Numerical simulations

To investigate the dynamics of the long cavity laser theoretically we consider the DDE model given by (2)-(3). We normalise the time variable t to the inverse filter bandwidth, obtaining $\gamma = 1$. The other dimensionless parameter values used in our simulations are $\gamma_g = 0.1$, $\tau = 1000$ with $\kappa = 0.2$ and $\alpha = 2$, where the pump parameter $g_0 = 1.7$ is chosen slightly above the lasing threshold $g_{0th} \approx -\log\kappa \approx 1.61$. We perform numerical simulations of this model and obtain a stable pulse train with several drops of electrical field intensity $|A(t)|^2$ per cavity round trip (see Fig. 6(a)).To demonstrate that the drops are heteroclinic connections between different stable modes in Fig. 6(b) we have zoomed the parts of the of intensity time trace around the plateau levels of approximately 1-4 lasing modes.

In order to study single drops in more detail, we show in Fig. 7(a) a stable solution with only one drop per cavity round trip by reducing linewidth enhancement factor α to 1.24. In Fig. 7(b) one can observe how the shape of the drop changes with time, demonstrating that the drop is not strictly periodic despite its regular appearance at each round-trip. Furthermore, from Fig. 8 we can see that the the solution of (2)-(3) is weakly chaotic and the orbit stays most of the time near the fourth stable lasing mode where the solution has a plateau. Note, that for the considered parameters only 22 modes are stable, other modes are unstable due to weak modulational instability [2], hence during the drop the trajectory performs an excursion around unstable modes similarly to the experiment.

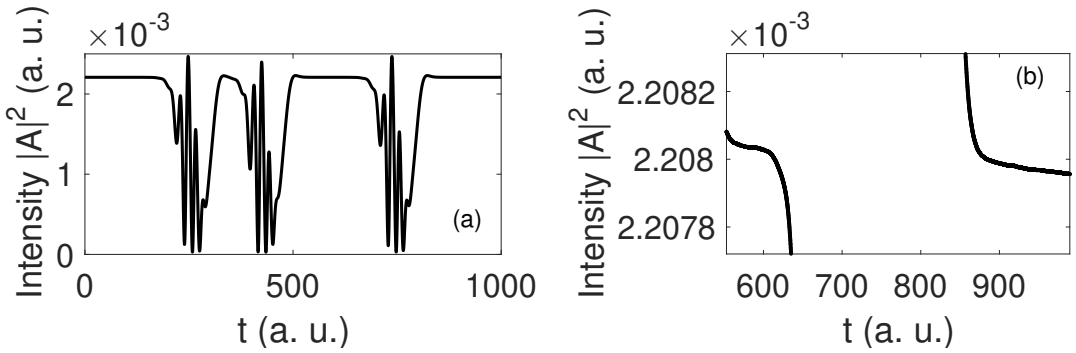

Figure 6: (a) Single round-trip of a stable solution with multiple drops during a round-trip. (b) Magnified difference between plateau levels of the solution at times $t \approx 600$ and $t \approx 1000$. Here, the difference between intensities of neighbouring lasing modes is around 1.6×10^{-7}, which accounts for the difference in plateau levels.

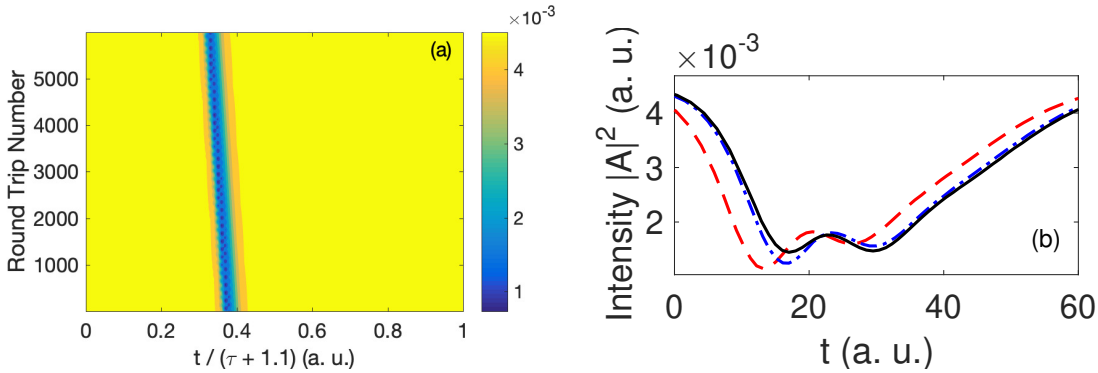

Figure 7: (a) Temporal evolution illustrating the sustainability of a single drop per round trip, $\alpha = 1.24$. (b) Shapes of the drop at different relative times: $t = t_0$ (solid black), $t = t_0 - 12\tau$ (blue dash-dotted), $t_0 - 18\tau$ (red dashed).

5 Conclusion

To conclude, we have experimentally demonstrated the formation of sustainable turbulent coherent localized structures in long cavity semiconductor lasers near the lasing threshold, which display irregular dynamics in their core. The long-term sustainability of the drops is due to the frequency of the drop being out of the filter transmission resonance, thus the SOA amplification at each roundtrip is counteracted by the losses induced by the filter. In other words, the sustainability is the result of a balance between the laser optical bandwidth and the non-linear dispersion. Numerically, we characterised the drops using DDE model, and demonstrated that such structures typically follow heteroclinic connections between two stable modes [8]. The drop corresponds to a weakly chaotic excursion around the unstable lasing modes resembling the evolution of Nozaki-Bekki holes. The results confirm the impact of the intra-cavity filter on the laser dynamics. In particular, the transmission bandwidth should be carefully considered when designing the laser for applications.

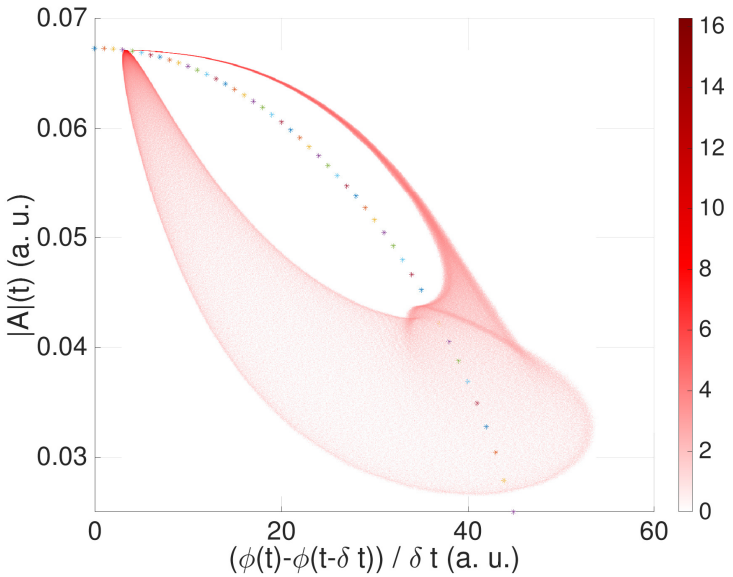

Figure 8: Weakly chaotic orbits of (2)-(3), where $\phi(t)$ is the phase of the field $A(t)$ and $\delta t = 5$. Stars denote various lasing modes. The color bar corresponds to the number of times the trajectory was near the point (log_{10}).

References

[1] E. Turitsyna, S. Smirnov, S. Sugavanam, N. Tarasov, X. Shu, S. Babin, E. Podivilov, D. Churkin, G. Falkovich, and S. Turitsyn, "The laminar–turbulent transition in a fibre laser," Nature Photonics, vol. 7, no. 10, p. 783, 2013.

[2] S. Slepneva, B. Kelleher, B. O'shaughnessy, S. Hegarty, A. Vladimirov, and G. Huyet, "Dynamics of fourier domain mode-locked lasers," Optics express, vol. 21, no. 16, pp. 19240–19251, 2013.

[3] S. Slepneva, B. O'Shaughnessy, A. G. Vladimirov, S. Rica, E. A. Viktorov, and G. Huyet, "Convective nozaki-bekki holes in a long cavity oct laser," Optics express, vol. 27, no. 11, pp. 16395–16404, 2019.

[4] T. Pfeiffer, M. Petermann, W. Draxinger, C. Jirauschek, and R. Huber, "Ultra low noise fourier domain mode locked laser for high quality megahertz optical coherence tomography," Biomedical optics express, vol. 9, no. 9, pp. 4130–4148, 2018.

[5] L. D. Landau, "On the problem of turbulence," in Dokl. Akad. Nauk USSR, vol. 44, p. 311, 1944.

[6] N. Bekki and K. Nozaki, "Formations of spatial patterns and holes in the generalized ginzburg-landau equation," Physics Letters A, vol. 110, no. 3, pp. 133–135, 1985.

[7] M. Bazhenov, T. Bohr, K. Gorshkov, and M. Rabinovich, "The diversity of steady state solutions of the complex ginzburg-landau equation," Physics Letters-Section A, vol. 217, no. 2, pp. 104–110, 1996.

[8] J. A. Sherratt, M. J. Smith, and J. D. Rademacher, "Patterns of sources and sinks in the complex ginzburg–landau equation with zero linear dispersion," SIAM Journal on Applied Dynamical Systems, vol. 9, no. 3, pp. 883–918, 2010.

[9] J. Lega, “Traveling hole solutions of the complex ginzburg–landau equation: a review,” Physica D: Nonlinear Phenomena, vol. 152, pp. 269–287, 2001.

[10] S. Popp, O. Stiller, I. Aranson, and L. Kramer, “Hole solutions in the 1d complex ginzburg-landau equation,” Physica D: Nonlinear Phenomena, vol. 84, no. 3-4, pp. 398–423, 1995.

[11] I. S. Aranson and L. Kramer, “The world of the complex ginzburg-landau equation,” Reviews of Modern Physics, vol. 74, no. 1, p. 99, 2002.

[12] J. Burguete, H. Chaté, F. Daviaud, and N. Mukolobwiez, “Bekki-nozaki amplitude holes in hydrothermal nonlinear waves,” Physical review letters, vol. 82, no. 16, p. 3252, 1999.

[13] N. Bekki, Y. Harada, and H. Kanai, “Bekki–nozaki hole in traveling excited waves on human cardiac interventricular septum,” Journal of the Physical Society of Japan, vol. 81, no. 7, p. 073801, 2012.

[14] A. Pimenov, S. Slepneva, G. Huyet, and A. G. Vladimirov, “Dispersive time-delay dynamical systems,” Physical review letters, vol. 118, no. 19, p. 193901, 2017.

[15] T. Kolokolnikov, M. Nizette, T. Erneux, N. Joly, and S. Bielawski, “The q-switching instability in passively mode-locked lasers,” Physica D: Nonlinear Phenomena, vol. 219, no. 1, pp. 13–21, 2006.

[16] B. Kelleher, D. Goulding, B. B. Pascual, S. P. Hegarty, and G. Huyet, “Phasor plots in optical injection experiments,” The European Physical Journal D, vol. 58, no. 2, pp. 175–179, 2010.